

# Conductivity and Hall effect measurements on intentionally undoped and doped AlGaIn/GaN heterostructures before and after passivation

J. Bernát, P. Javorka, M. Marso, and P. Kordoš<sup>a)</sup>

*Institute of Thin Films and Interfaces (ISG-1), Research Centre Jülich, D-52425 Jülich, Germany*

(Received 20 August 2003; accepted 3 November 2003)

Conductivity and Hall effect measurements were performed before and after Si<sub>3</sub>N<sub>4</sub> passivation of intentionally undoped and doped AlGaIn/GaN heterostructures on Si and SiC substrates. An increase of the sheet carrier density (up to ~30%) and a slight decrease of the electron mobility (less than 10%) are found in all samples after passivation. The passivation induced sheet carrier density is  $1.5\text{--}2 \times 10^{12} \text{ cm}^{-2}$  in undoped samples and only  $0.7 \times 10^{12} \text{ cm}^{-2}$  in  $5\text{--}10 \times 10^{18} \text{ cm}^{-3}$  doped samples. The decrease of the electron mobility after passivation is slightly lower in highly doped samples. The channel conductivity in both types of unpassivated samples on Si and SiC substrates increases with an increase in doping density. After passivation, a well-resolved increase of channel conductivity is observed in the undoped or lightly doped samples and nearly the same channel conductivity results in the highly doped samples. © 2003 American Institute of Physics.

[DOI: 10.1063/1.1637154]

It is well known that AlGaIn/GaN high-electron mobility transistors (HEMTs) exhibit significant radio-frequency (rf) dispersion<sup>1,2</sup> that is attributed to trapping effects caused mainly by surface states and partially by buffer/active-layer traps.<sup>2,3</sup> Surface passivation has been found to reduce current slump and microwave power degradation of intentionally undoped AlGaIn/GaN HEMTs.<sup>3</sup> However, the influence of passivation on device performance is not fully clear yet<sup>4</sup> and application of various insulators, mainly SiO<sub>2</sub> and Si<sub>3</sub>N<sub>4</sub>, is currently under detailed investigation. Mostly intentionally undoped devices are studied and an increase of carrier density in the channel is assumed on the basis of the drain current and increase in transconductance after passivation.<sup>3–8</sup> The only published Hall effect data show an increase of carrier density and a decrease of mobility, resulting in lower channel conductivity of undoped and doped AlGaIn/GaN heterostructures after SiO<sub>2</sub> passivation.<sup>9</sup> Recently, degradation of the rf performance after SiO<sub>2</sub> passivation and overall performance improvement after Si<sub>3</sub>N<sub>4</sub> passivation were observed.<sup>10</sup> Similar differences like an increase<sup>6</sup> or a decrease<sup>7</sup> of gate leakage current and an increase<sup>5</sup> as well as a decrease<sup>3,7</sup> of cut off frequencies of AlGaIn/GaN HEMTs after Si<sub>3</sub>N<sub>4</sub> passivation were reported. All these underscore the importance of further detailed studies of passivation in order to optimize the performance of GaN-based devices.

In this letter, we report on passivation-induced changes in the transport properties of AlGaIn/GaN heterostructures. Conductivity and Hall effect measurements before and after Si<sub>3</sub>N<sub>4</sub> passivation of heterostructures grown on Si and SiC substrates were performed. It is shown that the passivation has different impact on intentionally undoped and doped samples.

AlGaIn/GaN heterostructures were grown on high resistivity Si(111) and semi-insulating SiC substrates by metalorganic chemical vapor deposition. Intentionally undoped

structures consisted of 25 nm undoped AlGaIn (Si substrate) or 30 nm undoped AlGaIn and 3 nm undoped GaN cap (SiC substrate) grown on top of a GaN buffer. Doped structures consisted of a 5 nm undoped AlGaIn spacer, a 10 nm thick Si-doped AlGaIn carrier supply layer, and a 5 nm undoped AlGaIn barrier layer, grown on top of GaN buffer. The doping levels were  $2 \times 10^{18}$ ,  $5 \times 10^{18}$ , and  $1 \times 10^{19} \text{ cm}^{-3}$ . In the case of the  $1 \times 10^{19} \text{ cm}^{-3}$  doped structure on Si as well as structures on SiC a 3 nm undoped GaN cap was then grown. All AlGaIn layers have an Al content of  $x_{\text{AlIn}} \approx 0.28$ .

van der Pauw patterns with an active area of  $0.3 \times 0.3 \text{ mm}^2$  were processed simultaneously to the HEMT devices. Ohmic contact was prepared by evaporating layered Ti/Al/Ni/Au followed by annealing at 850 °C for 30 s in N<sub>2</sub> ambient. Room temperature conductivity and Hall effect measurements were performed on the same sample before and after Si<sub>3</sub>N<sub>4</sub> passivation. Plasma-enhanced chemical vapor deposition at 300 °C was used to prepare 100 and 150 nm thick Si<sub>3</sub>N<sub>4</sub> layer on samples with Si and SiC substrates, respectively. The layer thickness and refraction coefficient were controlled by ellipsometry. In some cases also  $\sim 5 \times 5 \text{ mm}^2$  samples with alloyed In contacts were used; the data obtained are consistent, within measurement error, with those found on patterned “small” samples.

TABLE I. Sheet carrier density, electron mobility, and sheet resistivity of AlGaIn/GaN heterostructures on Si substrates before and after passivation.

$N_D$ (cm <sup>-3</sup> )	Passivation	$n_s$ (10 <sup>12</sup> cm <sup>-2</sup> )	$\mu_n$ (cm <sup>2</sup> /V s)	$R_s$ (Ω/sq)
undoped	yes	7.12	1150	762
undoped	no	9.13	1080	631
$2 \times 10^{18}$	yes	7.98	1235	638
$2 \times 10^{18}$	no	9.81	1160	558
$5 \times 10^{18}$	yes	8.76	1173	610
$5 \times 10^{18}$	no	9.57	1093	579
$1 \times 10^{19}$	yes	9.20	1270	534
$1 \times 10^{19}$	no	9.86	1220	521

<sup>a)</sup>Electronic mail: p.kordos@fz-juelich.de

TABLE II. Sheet carrier density, electron mobility, and sheet resistivity of AlGaIn/GaN heterostructures on SiC substrates before and after passivation.

$N_D$ ( $\text{cm}^{-3}$ )	Passivation	$n_s$ ( $10^{12} \text{ cm}^{-2}$ )	$\mu_n$ ( $\text{cm}^2/\text{V s}$ )	$R_s$ ( $\Omega/\text{sq}$ )
undoped	yes	6.95	1930	466
undoped	no	8.21	1773	430
undoped	yes	7.77	1900	423
undoped	no	9.36	1725	387
$2 \times 10^{18}$	yes	9.32	1590	422
$2 \times 10^{18}$	no	10.2	1490	410
$5 \times 10^{18}$	yes	10.8	1430	404
$5 \times 10^{18}$	no	11.4	1355	405

The sheet carrier density, electron mobility, and sheet resistivity measured before and after passivation are shown in Tables I and II. The sheet carrier density in unpassivated samples is  $7\text{--}11 \times 10^{12} \text{ cm}^{-2}$  and it increases slightly with an increase in the level of doping. A well resolved increase of the carrier density after passivation is found in all samples investigated. The passivation-induced sheet charge decreases with an increase in the doping level from  $1.5\text{--}2 \times 10^{12} \text{ cm}^{-2}$  on undoped samples to  $0.7 \times 10^{12} \text{ cm}^{-2}$  on  $5\text{--}10 \times 10^{18} \text{ cm}^{-3}$  doped samples, as shown in Fig. 1. The relative change in sheet carrier density after passivation, shown in Fig. 2, confirms lower impact of passivation on samples with higher doping. The electron mobility in unpassivated samples on SiC substrates decreases with an increase in doping (from  $1900 \text{ cm}^2/\text{V s}$  on undoped samples to  $1430 \text{ cm}^2/\text{V s}$  on the  $5 \times 10^{18} \text{ cm}^{-3}$  doped sample) and in samples on Si substrates it is nearly the same ( $\mu_H \approx 1200 \text{ cm}^2/\text{V s}$ ). The influence of passivation on the electron mobility is less pronounced than that on the carrier density. Slightly lower mobilities than before passivation (less than a 10% decrease) were evaluated on all passivated samples (see Tables I and II). The relative change in mobility after passivation of intentionally undoped and doped samples is shown in Fig. 2.

Usually it is suggested that passivation of AlGaIn/GaN heterostructures reduces the surface trap density. According to our results, the number of electrons trapped on the unpassivated surface, which is proportional to the passivation-

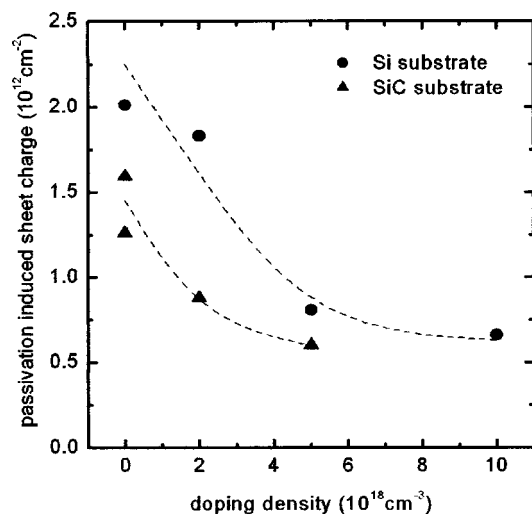


FIG. 1. Passivation-induced sheet carrier density in intentionally undoped and doped AlGaIn/GaN heterostructures grown on Si and SiC substrates. The lines are a guide for the eye.

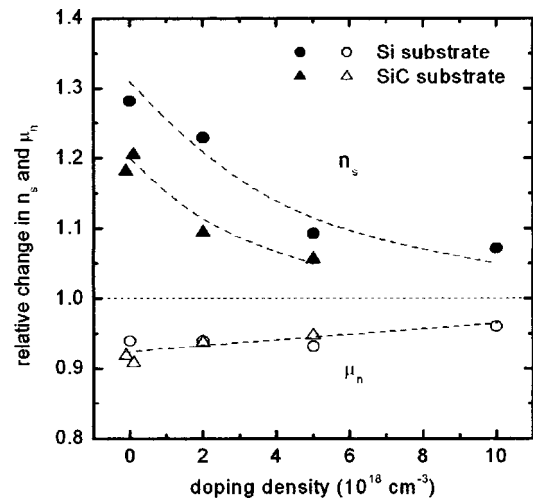


FIG. 2. Relative change in sheet carrier density and electron mobility of intentionally undoped and doped AlGaIn/GaN heterostructures after  $\text{Si}_3\text{N}_4$  passivation. The lines are a guide for the eye.

induced carrier density, decreases with an increase in the doping level. This conclusion can be supported by recent observations of unpassivated devices where the rf dispersion in doped AlGaIn/GaN HEMTs is significantly reduced in comparison to their undoped counterparts.<sup>11,12</sup> Another explanation for the results obtained can be made by considering stress-induced effects due to passivation. It is well known that deposition of dielectric layers like  $\text{SiO}_2$  and  $\text{Si}_3\text{N}_4$  produces residual stress that can range from tensile to compressive (up to  $\pm 1 \text{ GPa}$ ), depending on the process conditions.<sup>13</sup> Recently it was reported that passivation changes in AlGaIn/GaN HEMT performance can be explained by stress-induced polarization charge<sup>14</sup> and depend strongly on the amount of stress produced by different deposition conditions.<sup>15</sup> Thus, the passivation-induced increase of the sheet carrier density in the samples investigated follows from an additional piezoelectric field created by  $\text{Si}_3\text{N}_4$  passivation. Lower impact of passivation on more highly doped samples follows from the lower piezoresistivity of more highly doped samples.<sup>16</sup> The slightly different impact of passivation on the samples on Si and SiC substrates can be explained by differences in  $\text{Si}_3\text{N}_4$  thickness and thus by differences in stress induced.<sup>13</sup> Experiments to answer this question are in progress.

The channel conductivity of AlGaIn/GaN heterostructures on Si and SiC substrates before and after passivation is shown in Fig. 3. For unpassivated samples the channel conductivity increases with an increase in the doping density. After passivation, a well resolved increase of channel conductivity is observed on undoped or lightly doped samples, but nearly the same channel conductivity results on highly doped samples. From this it follows that the passivation impact on higher doped AlGaIn/GaN heterostructures is less pronounced than on undoped or lightly doped ones.

In conclusion, we performed conductivity and Hall effect measurements on intentionally undoped and doped AlGaIn/GaN heterostructures before and after passivation. An increase of the sheet carrier density (up to  $\sim 30\%$ ) and a slight decrease of the electron mobility (less than 10%) were found for all samples after passivation. The passivation-induced sheet carrier density is  $1.5\text{--}2 \times 10^{12} \text{ cm}^{-2}$  on un-

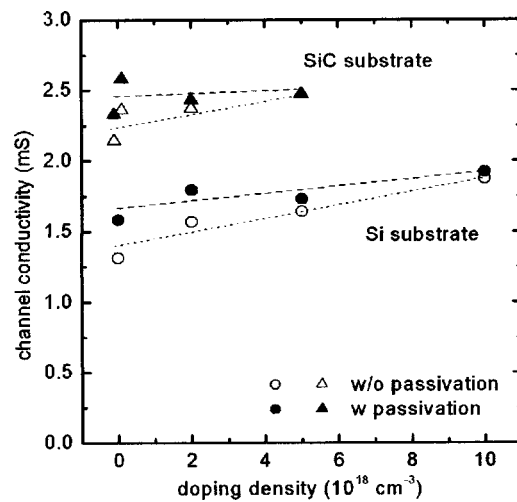


FIG. 3. Impact of  $\text{Si}_3\text{N}_4$  passivation on the channel conductivity in intentionally undoped and doped AlGaIn/GaN heterostructures grown on Si and SiC substrates. The lines are a guide for the eye.

doped samples and only  $0.7 \times 10^{12} \text{ cm}^{-2}$  on  $5\text{--}10 \times 10^{18} \text{ cm}^{-3}$  doped samples. The channel conductivity of undoped or lightly doped samples increases after passivation, but nearly the same channel conductivity results on highly doped samples.

The authors thank Y. Dikme of the Technical University of Aachen and M. Heuken of AIXTRON AG, Aachen, for

samples on Si substrates and J. Flynn and G. Brandes of ATMI for samples on SiC substrates.

- <sup>1</sup>S. C. Binari, W. Kruppa, H. B. Dietrich, G. Kelner, A. E. Wickenden, and J. A. Freitas, *Solid-State Electron.* **41**, 1549 (1997).
- <sup>2</sup>S. Trassaert, B. Boudart, C. Gaquiere, D. Theron, Y. Crosnier, F. Huet, and M. A. Poisson, *Electron. Lett.* **35**, 1386 (1999).
- <sup>3</sup>B. M. Greene, K. K. Chu, E. M. Chumbes, J. A. Smart, J. R. Shealy, and L. F. Eastman, *IEEE Electron Device Lett.* **21**, 268 (2000).
- <sup>4</sup>G. Koely, V. Tilak, L. F. Eastman, and M. G. Spencer, *IEEE Trans. Electron Devices* **50**, 886 (2003).
- <sup>5</sup>I. Harrison, W. Clayton, and W. Jeffs, *Phys. Status Solidi A* **188**, 275 (2001).
- <sup>6</sup>W. S. Tan, P. A. Houston, P. J. Parbrook, G. Hill, and R. J. Airey, *J. Phys. D* **35**, 595 (2002).
- <sup>7</sup>W. Lu, V. Kumar, R. Schwindt, E. Piner, and I. Adesida, *Solid-State Electron.* **46**, 1441 (2002).
- <sup>8</sup>B. Luo, R. Mehandru, J. Kim, F. Ren, B. P. Gila, A. H. Onstine, C. R. Abernathy, S. J. Pearson, R. Fitch, J. Gillespie, T. Jenkins, J. Sewell, D. Via, A. Crespo, and Y. Irokawa, *J. Electrochem. Soc.* **149**, G613 (2002).
- <sup>9</sup>X. Z. Dang, E. T. Yu, E. J. Piner, and B. T. McDermott, *J. Appl. Phys.* **90**, 1357 (2001).
- <sup>10</sup>P. Javorka, J. Bernát, A. Fox, M. Marso, H. Lüth, and P. Kordoš, *Electron. Lett.* **39**, 1155 (2003).
- <sup>11</sup>O. Mitrofanov, M. Mandra, and N. Weimann, *Appl. Phys. Lett.* **82**, 4361 (2003).
- <sup>12</sup>J. Bernát, P. Javorka, A. Fox, M. Marso, H. Lüth, and P. Kordoš, *Solid-State Electron.* **47**, 2097 (2003).
- <sup>13</sup>S. M. Hu, *J. Appl. Phys.* **70**, R53 (1991).
- <sup>14</sup>A. Conway, P. Asbeck, and J. Moon, 45th Electronic Material Conference, Salt Lake City, UT, June 2003, Abstracts book, TMS, p. 85.
- <sup>15</sup>W. S. Tan, P. A. Houston, G. Hill, M. W. Low, P. J. Parbrook, and R. J. Airey, in Ref. 14, p. 84.
- <sup>16</sup>M. Eickhoff, O. Ambacher, G. Krötz, and M. Stutzmann, *J. Appl. Phys.* **90**, 3383 (2001).